Detailed dynamic thermal-hydraulic network model

Application to liquid-immersed power transformers

Zoran Radaković, Marko Novković,
Patrick Picher, Federico Torriano

ABSTRACT

The paper presents the concept of temperature calculation in oil-immersed power transformers based on a detailed Thermal-Hydraulic Network Model (THNM). The THNM is deeply rooted in physics, incorporating detailed construction, material properties, and cooling equipment characteristics. Software tools based on a steady-state version of detailed THNM are becoming prevalent as design tools. However, a detailed dynamic THNM has not yet reached that level of technology readiness. Its practical application lies in operational decision-making, grid planning, and investment planning, as well as monitoring, where the detailed dynamic THNM can be used to simulate transformer thermal behavior during grid operation under variable loading conditions.

KEYWORDS:

Thermal-hydraulic network model, transformer loading, transient thermal analysis, digital twin

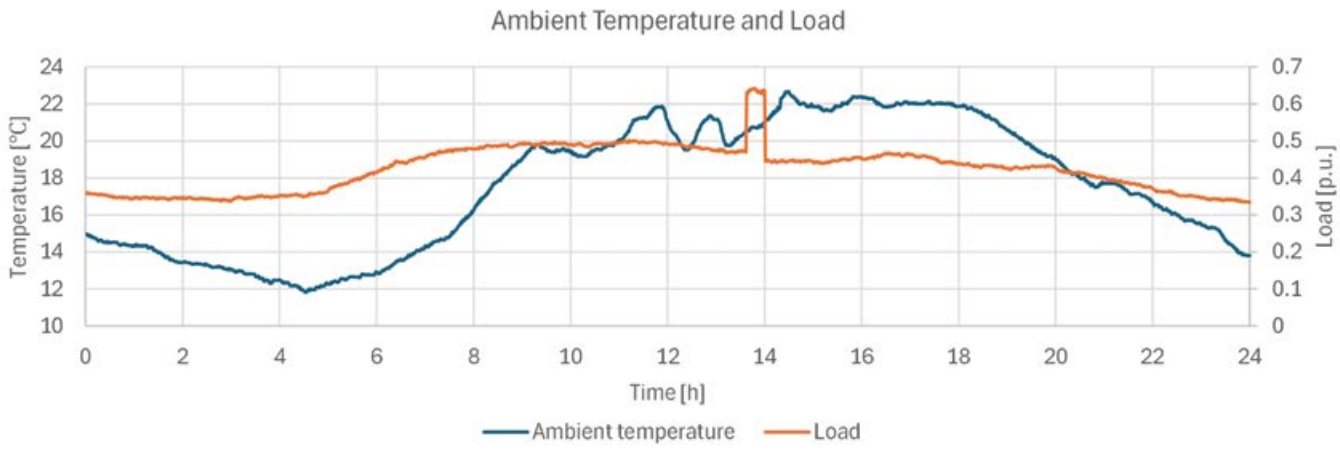
Ambient Temperature and Load
Temperature [°C]
Load [p.u.]
Time [h]
Ambient temperature
Load

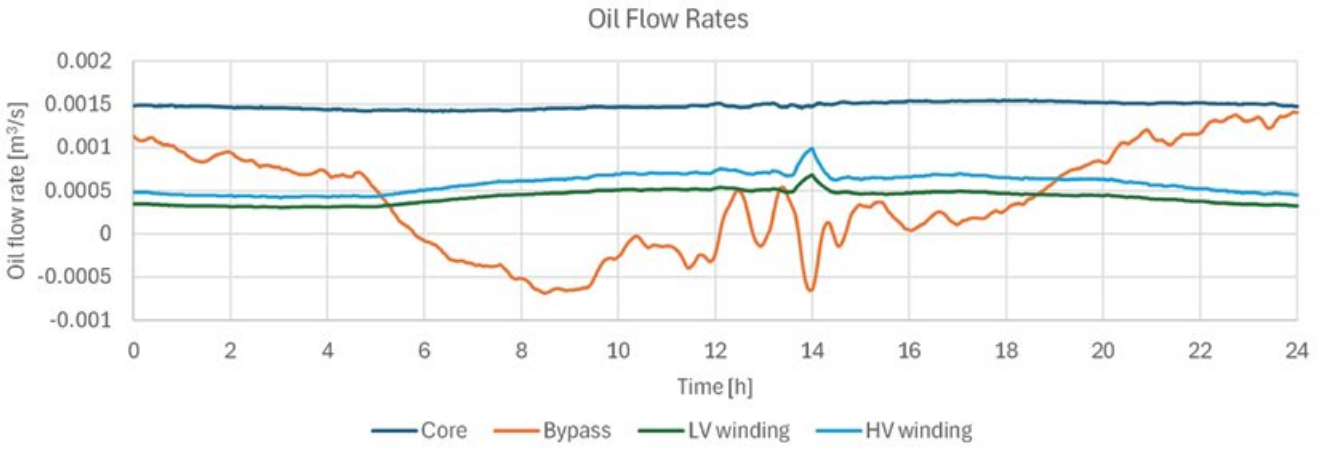
Oil Flow Rates
Oil flow rate [m³/s]
Time [h]
Core
Bypass
LV winding
HV winding

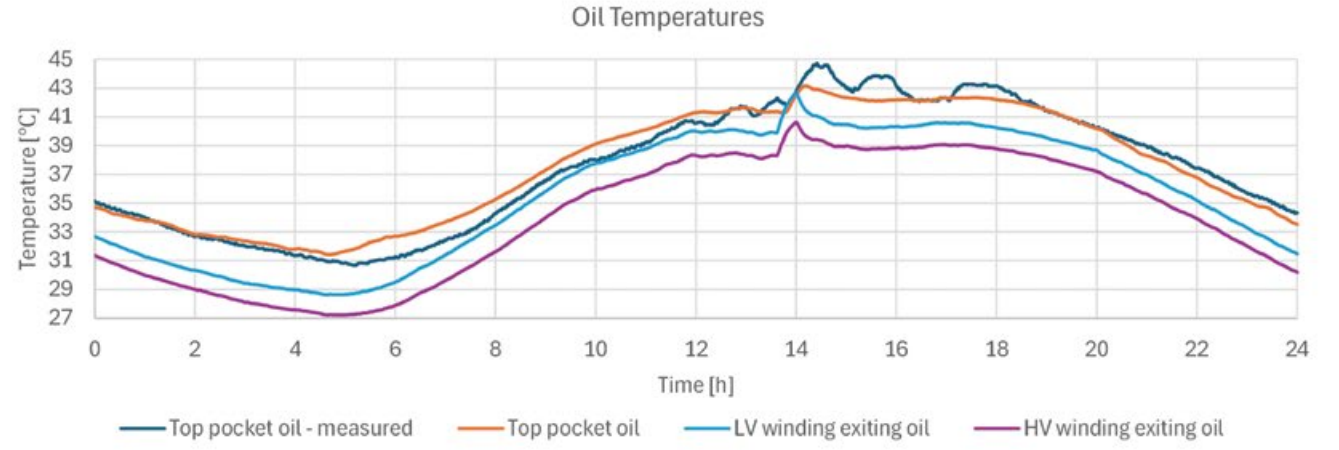
Oil Temperatures
Temperature [°C]
Time [h]
Top pocket oil - measured
Top pocket oil
LV winding exiting oil
HV winding exiting oil

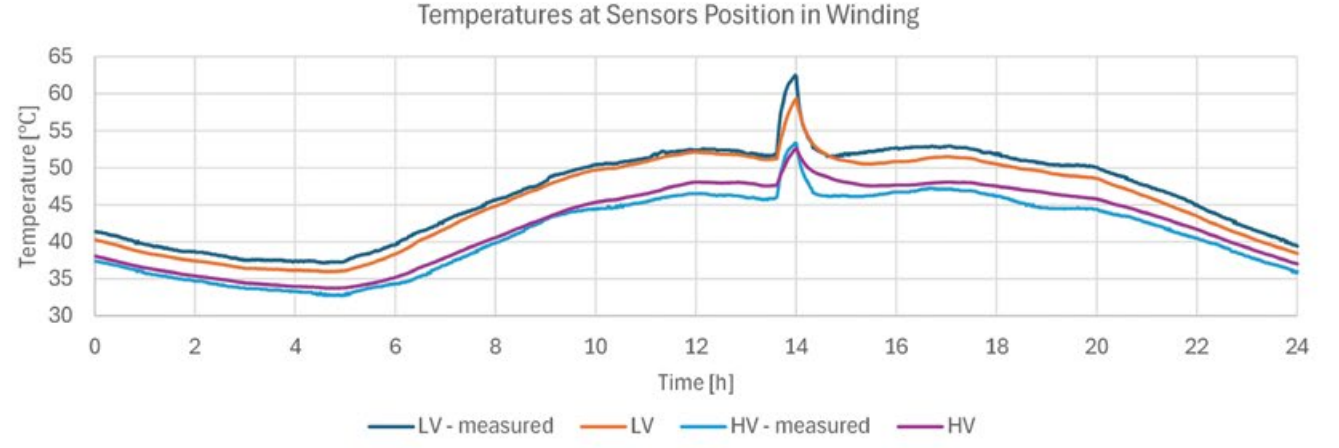
Temperatures at Sensors Position in Winding
Temperature [°C]
Time [h]
LV - measured
LV
HV - measured
HV

1. Introduction

The temperature inside the tank of liquid-immersed power transformers (LIPTs) is a limiting factor for transformer loading. Immediate failure appears if the temperature exceeds a certain level, depending on the material characteristics. A temperature increase above the rated material limit causes accelerated aging, resulting in transformer loss of life.

Characteristic temperature rises are verified through factory temperature-rise tests. Typically, the winding and oil temperature rises are measured under steady-state rated load conditions. Temperature calculations are performed during the LIPTs design process to ensure that the produced transformer complies with these test requirements.

Extended temperature-rise tests, including short-time overloads, may also be specified by agreement. In such a case, transient thermal process calculations are needed during the LIPT design stage.

The temperatures change during the LIPT grid operation. It is caused by different reasons, as stated in Chapter 2. Chapter 3 outlines the practical planning and monitoring aspects that require temperature calculation during transient thermal processes.

Temperature calculation is particularly challenging due to the complex construction of LIPTs, and the intricate interplay of fluid dynamics and heat transfer phenomena. The different approaches are available, as systematically presented in [1]. The approach based on a detailed dynamic THNM requires detailed data on transformer construction, the physical properties of the materials used, and the characteristics of the cooling equipment. No measurements are required for model parameterization. On a computer equipped with an AMD Ryzen 7 7700X CPU (eight cores, base clock 4.5 GHz), the current computational time is approximately one-third of the duration of the corresponding real transient thermal process, with potential for further acceleration.

After developing the steady-state version of THNM (the basics of which are described in [2], published in 2010) and implementing it in a software design tool [3], we developed a dynamic version of THNM. The first publication about it was in 2023. The extension of the steady-state THNM to a dynamic THNM is presented in several publications from 2023, as stated in our last paper [4]. In [4], the model is validated using two sets of data: (1) 7 days of winter and 7 days of summer operation from a three-phase 225/26.4 kV, YNd1, 66 MVA transformer, and (2) a 60-hour extended temperature-rise test from a single-phase 424.35/181.87 kV, 370 MVA transformer.

The approach based on a detailed dynamic THNM requires detailed data on transformer construction, the physical properties of the materials used, and the characteristics of the cooling equipment

The paper demonstrates the application of dynamic THNM for resolving practical tasks.

Since the Thermal-Hydraulic Network Model (THNM) requires detailed transformer construction data, close collaboration between transformer manufacturers and the provider of the dynamic THNM software is essential to ensure accurate modeling.

2. Variable parameters influencing the temperature in grid operation

In grid operation, both the load and the temperature of the external cooling medium fluctuate, leading to corresponding variations in transformer internal temperatures. Some simpler models, widely used in practice, calculate temperature rises independently of the cooling medium temperature. Temperatures are then obtained by adding these temperature rises to the cooling medium temperature. This approach does not account for the significant influence of viscosity, which varies strongly with temperature. In contrast, the dynamic THNM incorporates the temperature dependence of the liquid's viscosity.

The THNM considers the influence of the on-load tap changer (OLTC) position. It relates not only to considering the currents and conductors loaded with current at different OLTC positions, but also to the distribution of magnetic leakage flux, which varies with the OLTC position. Two-dimensional FEM Andersen's software was used for the calculations of the distribution of eddy and DC losses for different OLTC positions. The losses are recalculated for the temperature of each conductor.

Moreover, the dynamic THNM responds to any changes in the cooling system. It models the local influences of each fan or radiator. Even a small change in the cooling system, such as the change of the position of a reserve (inactive) fan or radiator, will affect the temperatures. The THNM also accounts for the eventual changes in pump operating status. By considering the local influence of each fan, the model covers changes in all AF cooling modes, with the ON/OFF status of each fan serving as an input parameter.

The equations of the detailed THNM are based on the following fundamental principles: a) conservation of heat, b) conservation of mass, and c) pressure equilibrium in closed loops

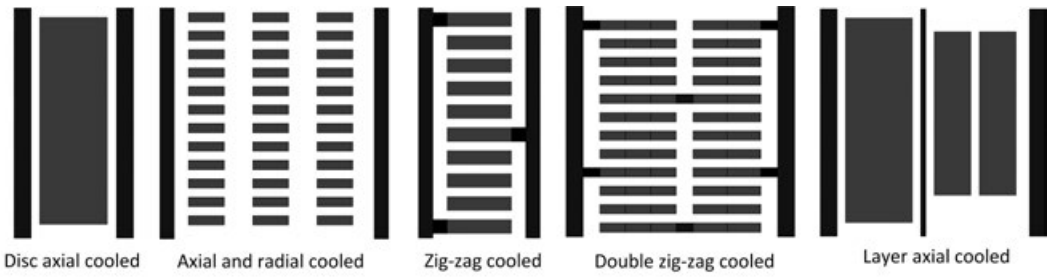

Winding types

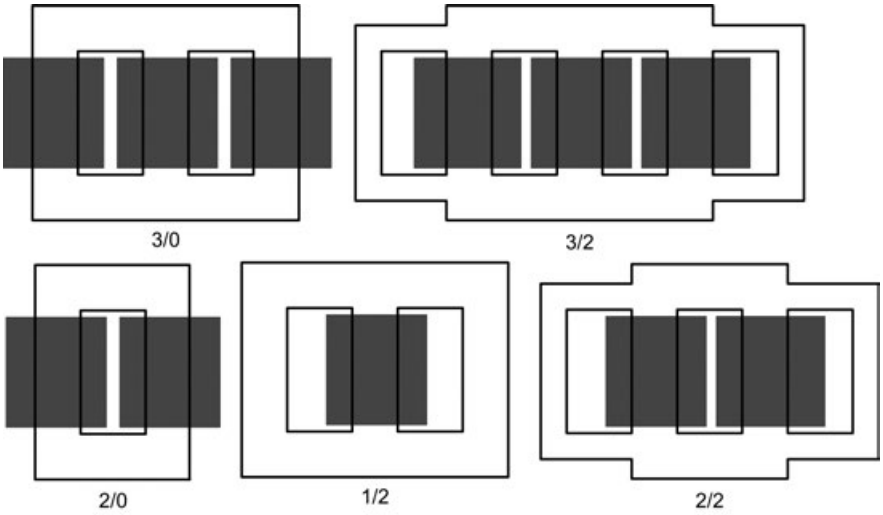

Core shapes

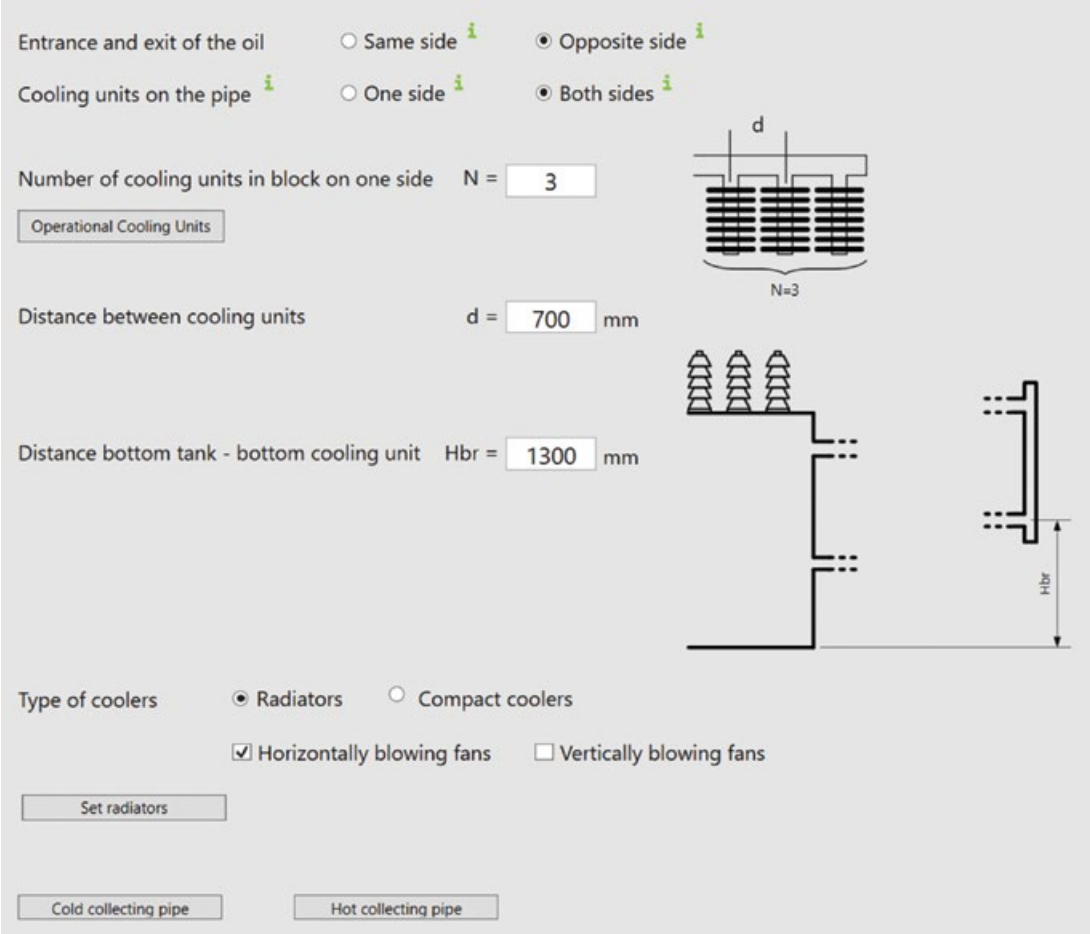

Cooling system

Figure 1. Some examples of construction covered by the HoST Calculus software

3. The role of temperature calculation in practice

Due to the high thermal inertia of large LIPTs, they can be temporarily loaded beyond their nameplate rating, as noted in loading guides such as [5]. This capability provides opportunities for improved protection, monitoring, and planning in the operation of LIPTs.

It is possible to operate LIPTs with regular (repeatable) periods of loading over the nameplate power. In such cases, the aging of LIPT should be estimated by calculation, to ensure it does not exceed the planned level (typically, a cumulative relative aging should be below 1). Furthermore, the monitoring system must track the hottest insulation (insulation hot spot) temperature, liquid temperature, and load to ensure compliance with the limits defined in transformer loading guidelines.

The software serves as a valuable tool for determining whether an existing unit should be replaced or if an additional unit needs to be installed.

At a more advanced level, thermal and aging calculations can be used to evaluate scenarios involving anticipated load increases and to support decision-making regarding grid reconfiguration to alleviate transformer overload.

Another critical consideration is the management of short-term overloads during emergencies caused by grid element outages. For grid operators, it is essential to understand both the magnitude and duration of overload that an LIPT can withstand. Access to this information supports informed decision-making when reconfiguring the grid in response to such events.

4. Basics of detailed THNM

The equations of the detailed THNM are based on the following fundamental principles: a) conservation of heat, b) conservation of mass, and c) pressure equilibrium in closed loops. The equations are generated and solved automatically for both the hydraulic and thermal networks. These networks are generated automatically based on the given transformer construction. The hydraulic and thermal models are two-dimensional in both static and dynamic THNMs. The implementation of the thermal models differs between static and dynamic THNMs, as presented in [2] for static THNM and [4] for dynamic THNM. In the static THNM, two-dimensional (radial and axial dimensions) network models are built and solved. The dynamic THNM is based on the convection-diffusion equation, more specifically on its discrete form. A consideration of the second dimension in the thermal model is achieved by boundary conditions at the spatial element ends. The temperature of the mixed oil is calculated at the position where it occurs.

Through an iterative process, the THNM delivers: a) the global distribution of oil flow and its temperatures at the inlet and outlet of the transformer parts (winding, core, and cooling equipment), b) the distribution of the flows within these parts and the oil temperature in each duct, c) the temperature of each conductor in the windings, d) hot-spot and surface temperatures of the core.

The deeply physics-rooted model accounts for all influencing parameters stated in Chapter 1 (the load, the temperature of the external cooling medium, the influence of oil viscosity, the on-load tap changer position, the distribution of magnetic leakage flux for specific tap positions, the active states of pumps, radiators, and fans). The software [3] covers a wide range of practical transformer constructions. Fig. 1 illustrates some examples for the windings, core shape, and the cooling system (there are options of the radiators and compact coolers, both of them connected to the tank by the collecting pipes (the case presented in the Fig. 1) or directly to the tank. The system guiding the oil into OD cooled windings can be specified. Chapter 5.1 shows some input data to illustrate the construction details considered by dynamic THNM.

The deeply physics-rooted model accounts for all influencing parameters such as the load, the temperature of the external cooling medium, the influence of oil viscosity, the on-load tap changer position, etc.

5. Resolving practical tasks

5.1 Briefly about test transformers

The analyses are based on data on two LIPTs with natural oil circulation, both equipped with fiber-optics sensors.

The first LIPT is a three-phase unit with a rated power 40/53/66 MVA for ONAN/ONAF1/ONAF2 cooling modes, operated on the grid. During the winter period, from February 3 to 9, 2023, the cooling mode varied (ONAN/ONAF1/ONAF2). During the summer period, July 18 – August 4, 2023, it was operated with all fans on (ONAF2). Ambient temperatures exceeded 20°C in summer, and dropped below 0°C in winter, with extreme lows below -25°C. The OLTC position also varied during operation.

The second LIPT is a single-phase 370 MVA unit with ONAF cooling. Results from the extended temperature-rise test were available. The tests were performed on the short-circuited transformer, with sharp step-up and step-down current changes. This enables the investigation of the temperature difference between the hot-spot and the mixed bulk top-oil, which is explicitly incorporated as a component in the thermal model defined in the current IEC loading guide [5].

Model parameters, presented in Table 1 for the IEC standard [5] and IEEE Annex G standard [6], were determined from the simulation results of HoST calculus software [3] for the 66 MVA transformer, using ambient temperatures 30°C (summer parameters) and -10°C (winter parameters). For the 370 MVA transformer, the parameters (Table 2) were obtained at an ambient temperature of 20°C, corresponding to the conditions of the extended temperature-rise test. All parameters are given for the rated operating point: $\Theta_{to,rated}$ is top-oil (mixed bulk

For long-term emergency loading, guide [5] states the following limits: a maximum load of 1.5 p.u. (in respect to rated power), a maximum hot-spot temperature of 140 °C, and a maximum top bulk oil of 105 °C

top-oil) temperature rise, $\Delta\Theta_{hs,to}$ is hot-spot temperature minus top-oil temperature (for both LV and HV windings), $\Delta\Theta_{a,ao}$ is average winding temperature minus average oil temperature (for both LV and HV windings), $\Theta_{bo,rated}$ is bottom-oil temperature rise, and H is hot-spot factor, being equal to $H = \Delta\Theta_{hs,to} / \Delta\Theta_{a,ao}$ (for both LV and HV windings). The model from the IEEE Annex G standard [6] requires the ratio of eddy losses to DC losses at the hot-spot position E_{HS}. To get it, it is necessary to calculate the losses distribution over the winding. The factor E_{HS} is then obtained by dividing the calculated eddy losses by the calculated DC losses at the hot-spot position. The winding-to-oil temperature gradient $\Delta\Theta_{a,ao}$ in the HV and LV windings exhibits significant discrepancies, indicating a deviation from sound engineering design principles. The situation with $\Delta\Theta_{hs,to}$ temperature difference is even worse due to the difference in the hot-spot factors H. This transformer serves as an example of suboptimal thermal design and was consequently analyzed by CIGRE Working Group A2.38 [7]. Notably, this transformer was designed using classical engineering tools, which likely contributed to the observed thermal performance issues.

The vertical position of the hot spot, required in [6], H_H is obtained from the simulation results of HoST calculus software [3].

For the IEEE Annex G model, the H_H has values 1 for the LV and 103/104 for HV winding of 66 MVA transformer, and values 1 for the LV and 143/144 for HV winding of 370 MVA transformer. E_{HS} is 1.6845 and 0.1040 for the LV and HV windings of 66 MVA transformer, and 1.1259 and 0.5771 for the LV and HV windings of 370 MVA transformer.

For the other parameters of the IEC model and IEEE Annex G model, typical values from the Standards are used.

A winding time constant of 7 minutes is used for the IEC model, and of 5 minutes for the IEEE Annex G model. For the IEC model, the following typical values were used: $x = 0.8$; $y = 1.3$; $K_{11} = 0.5$; $K_{21} = 2$, $K_{22} = 2$, and an oil time constant of 150 minutes for both transformers. For the losses ratio R, for 66 MVA transformer 7.21 was used, and for 370 MVA transformer 10^9 is used in order to simulate a short-circuited transformer. For the IEEE Annex G model, the following typical values were used: for ONAF cooling mode $x = 0.5$; $y = 0.9$; $z = 0.5$; and for ONAN cooling mode $x = 0.5$; $y = 0.8$; $z = 0.5$.

5.2 Estimation of the aging in normal cycling load

The load of LIPTs can, during certain periods, exceed the rated load. Standard [5] defines the limits for different kinds of overloading. For long-term emergency loading, guide [5] states the following limits: a maximum load of 1.5 p.u. (in respect to rated power), a maximum hot-spot temperature of 140 °C, and a maximum top bulk oil of 105 °C.

Ambient temperatures of the 66 MVA LIPT for one-week periods in winter and summer are shown in Fig. 2. A sample of the per-unit load (with respect to the rated power 66 MVA) dataset used for the analysis in this chapter is shown in Fig. 3.

Table 1. The parameters of the 66 MVA transformer obtained by the HoST Calculus software

Parameter	Winter parameters			Summer parameters		
	ONAN	ONAF1	ONAF2	ONAN	ONAF1	ONAF2
$\Theta_{to,rated}$	50.92	46.34	49.44	49.59	43.97	46.86
$\Delta\Theta_{hsLV,to}$	21.68	37.16	55.56	20.81	33.23	49.84
$\Delta\Theta_{hsHV,to}$	9.58	14.76	24.96	10.21	18.53	22.84
$\Delta\Theta_{aLV,ao}$	9.55	17.61	27.24	10.15	17.68	27.54
$\Delta\Theta_{aHV,ao}$	4.74	9.77	15.90	5.49	10.65	16.79
$\Theta_{bo,rated}$	24.40	15.73	13.68	29.58	21.50	19.59
H_{LV}	2.27	2.11	2.04	2.05	1.88	1.81
H_{HV}	2.02	1.51	1.57	1.86	1.74	1.36

Table 2. The parameters of the 370 MVA transformer obtained by the HoST Calculus software

Parameter	Calculated parameters
$\Theta_{to,rated}$	45.04
$\Delta\Theta_{hsLV,to}$	34.96
$\Delta\Theta_{hsHV,to}$	26.06
$\Delta\Theta_{aLV,ao}$	17.93
$\Delta\Theta_{aHV,ao}$	14.09
$\Theta_{bo,rated}$	15.56
H_{LV}	1.95
H_{HV}	1.85

Monitoring data obtained by a sensor, based on capacitive technology, indicates a low moisture content. Therefore, transformer aging was calculated according to [5] for a low moisture content of 0.5 %.

The relative aging for the following four load cases is presented: 1) weekly load and ambient temperature in winter, 2) weekly load and ambient temperature in summer, 3) weekly winter load scaled by a factor of 1.18, and 4) weekly summer load scaled by a factor of 2.73, resulting in a peak load equal to 1.41 p.u. (peak of scaled winter load 3). The winter load was increased until one of the long-term emergency loading limits from Guide [5] was reached. At a scale factor of 1.18, the temperature at the sensor location in the LV winding reached 140°C. For this scaling factor, the peak load is equal to 1.41.

The changes of the hot-spot temperatures in HV and LV windings for cases 1) to 4) are presented in Figs 4 to 7, respectively. The red dotted line (scale on the right vertical axis) represents the position of the hottest disk. The LV winding contains 78 discs, while the HV winding contains 104 discs. The position of the hottest disc changes over time.

Due to the changing position of the hottest disc, aging is calculated using temperatures from the dynamic THNM, which is calculated for all discs with the temperature of the hottest disc at any

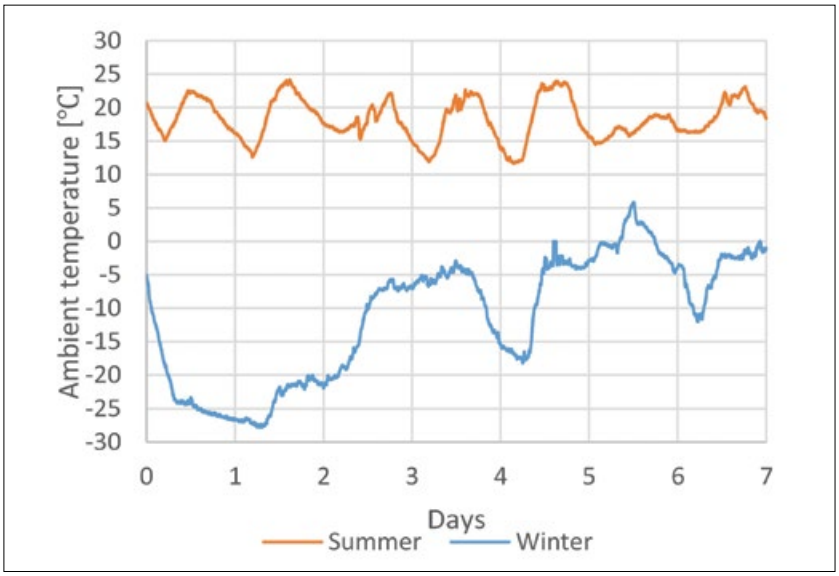

Figure 2. Ambient temperature in summer and winter weeks

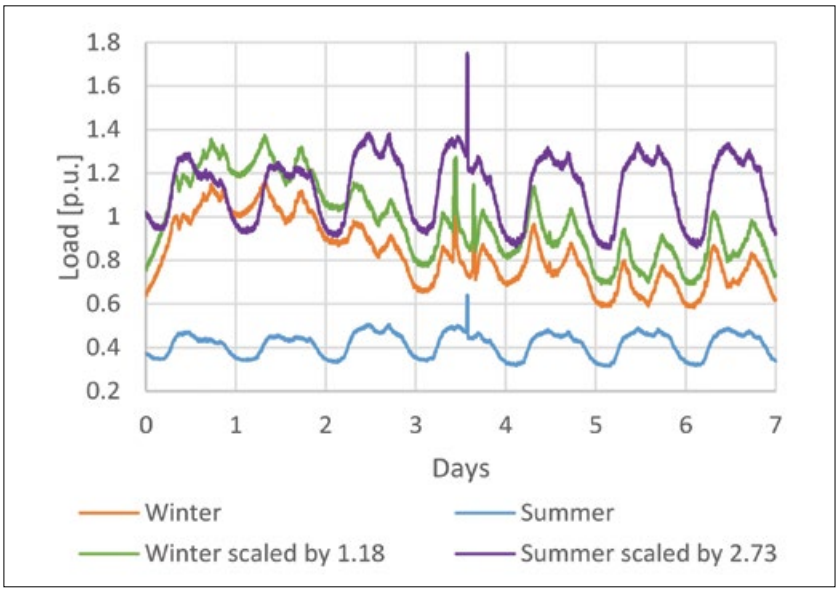

Figure 3. Per unit load during summer and winter weeks

The LV winding contains 78 discs, while the HV winding contains 104 discs, and the position of the hottest disc changes over time

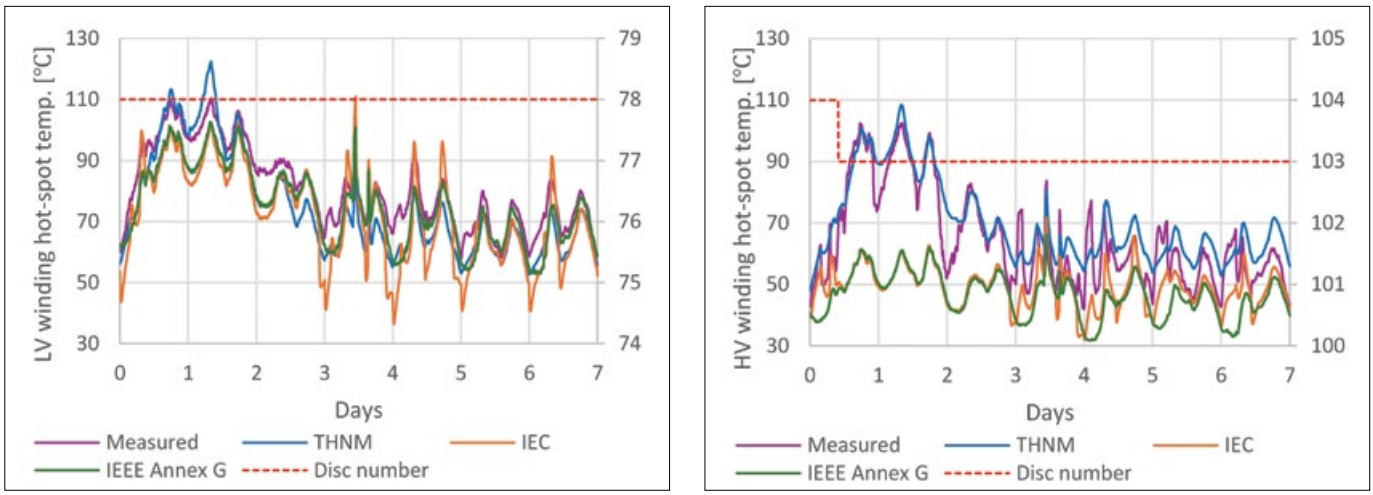

Figure 4. Hot-spot temperature change during winter for case 1) – for the LV winding (left), and for the HV winding (right)

Due to the changing position of the hottest disc, aging is calculated using temperatures from the dynamic THNM, which is calculated for all discs with the temperature of the hottest disc at any time instance

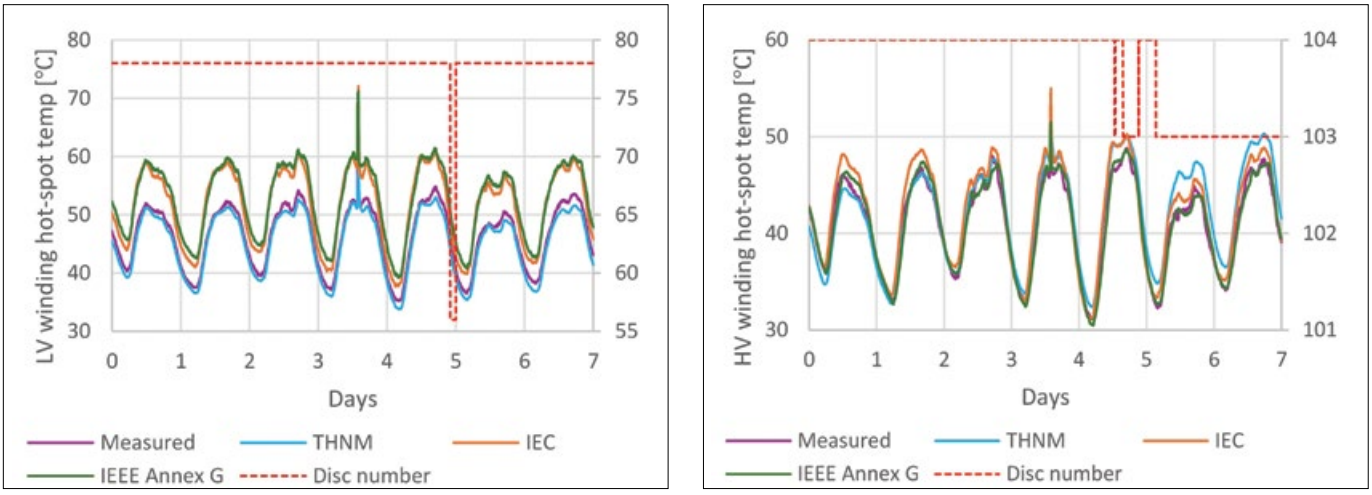

Figure 5. Hot-spot temperature change during summer for case 2) – for the LV winding (left), and for the HV winding (right)

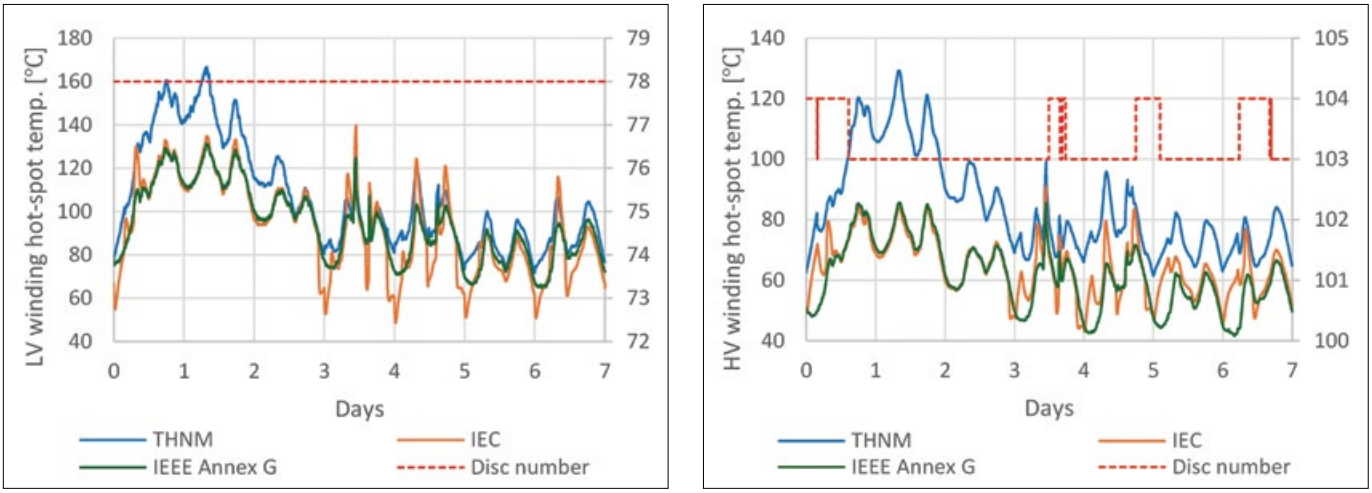

Figure 6. Hot-spot temperature change during winter for case 3) – for the LV winding (left), and for the HV winding (right)

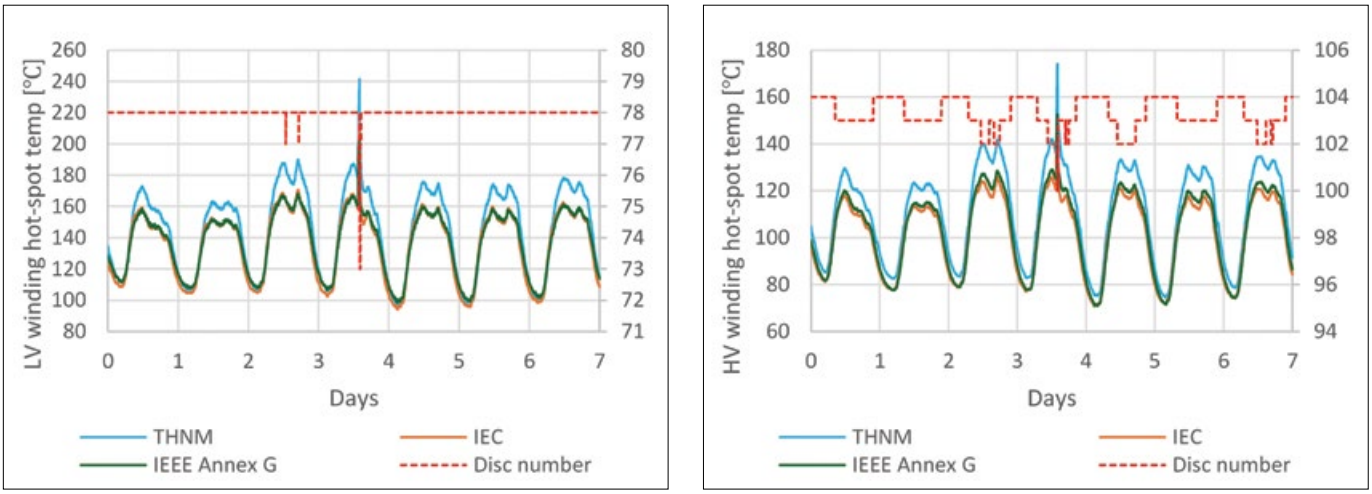

Figure 7. Hot-spot temperature change during summer for case 4) – for the LV winding (left), and for the HV winding (right)

time instance. The values presented in Table 3 correspond to the disc with the highest relative aging. For example, the aging for Load 4), for discs 102, 103, and 104 in HV winding amounts 13.2, 13.66, and 9.73, respectively. The LV winding experiences higher temperatures; thus, all values for maximum hot-spot temperature and relative aging in Table 3 refer to the LV winding. The values of the aging in the rows "Measured" are calculated from the temperatures measured by a fiber optics sensor positioned between discs 75 and 76. In the rows "THNM (hot-spot, disc 78)", the aging is calculated using the highest calculated temperature (of disc 78). In the rows "average discs 75 and 76", the aging is calculated using the average calculated temperature of discs 75 and 76). During the winter (Load 1), the difference between the real hot-spot (disc 78) and the temperature at the sensor's position (spacer between discs 75 and 76) becomes significant. In Figure 14 in [4], a comparison between calculated temperatures in disc 78 and calculated average temperature of discs 75 and 76 is presented for Load 1): the maximum difference is 34.71°C. Please note that on the graphics in [4], values of the hot-spot calculated by THNM at the position of the temperature sensor (corresponding to rows THNM (average discs 75 and 76) are used for the comparison of the hot-spot temperatures with their measured values. The maximum calculated temperature at the position of the sensor is 122.41°C, while the maximum temperature registered by the sensor is 110.38°C. The maximum difference between calculated temperatures in disc 78 and calculated average value of the maximum temperatures in discs 75 and 76 for Load 2) amounts to 4.61°C, and this is in line with the small difference between the maximum hot-spot temperatures for "THNM" (63.69°C) and "measured" (62.48°C) for Load 2). The thermal-hydraulic behavior of the system varies with load and ambient temperature, with ambient temperature showing a dominant influence. At lower ambient temperatures (with higher load), increased oil viscosity leads to uneven flow distribution through the radial ducts, with most of the oil passing through a few bottom ducts. This results in a significant temperature rise at the top of the pass. In contrast, at higher ambient temperatures (with lower load), lower oil viscosity enables a more uniform flow through all radial ducts, leading to a more balanced temperature distribution across the pass (discs 75 - 78).

The overshoot in the hot-spot to bulk top-oil temperature difference strongly depends on the micro-location of the temperature sensor measuring the bulk top-oil temperature

5.3 Behavior for step load increase

The dynamic THNM [4], as well as the Annex G IEEE [6] and IEC [5] models, were validated through extended temperature-rise tests with step current changes on a 370 MVA LIPT [4]. It has been shown that there is no overshoot in the hot-spot

Table 3. Characteristic temperature and estimated relative aging for different loading scenarios

	Max load [p.u.]		Max hot-spot temp. [°C]	Max top-oil temp. [°C]	Ageing [days]
Load 1) Winter	1.19	THNM (hot-spot, disc 78)	155.23	44.07	7.2711
		THNM (average discs 75 and 76)	122.41	44.07	0.5044
		IEC	110.93	49.01	0.1685
		Annex G IEEE	102.64	39.72	0.1775
		Measured	110.38	46.48	0.3992
Load 2) Summer	0.52	THNM (hot-spot, disc 78)	63.69	43.52	0.0016
		THNM (average discs 75 and 76)	59.32	43.52	0.0013
		IEC	72.10	41.79	0.0035
		Annex G IEEE	71.23	41.31	0.0039
		Measured	62.48	44.87	0.0015
Load 3) Winter	1.41	THNM	166.65	55.73	33.4047
		IEC	139.68	63.00	3.5257
		Annex G IEEE	131.44	52.21	2.7030
		Measured	/	/	/
Load 4) Summer	1.41	THNM	241.53	113.27	582.0841
		IEC	213.11	99.48	155.8942
		Annex G IEEE	201.89	102.56	145.5381
		Measured	/	/	/

Table 4. Maximum hot-spot temperatures and relative aging for different step-up loads

Load	THNM	Annex G of IEEE [6]	IEC [5]	Tables in [8]
0.5, 1.7, 1h	129.91/0.36	131.81/0.53	162.75/7.20	135/0.875
0.8, 1.5, 1h	118.83/0.24	123.09/0.41	143.24/1.86	128/0.641
0.5, 1.5, 2h	130.19/0.74	128.99/0.73	148.78/6.04	134/1.37
0.9, 1.4, 2h	128.48/1.10	127.28/1.22	138.57/3.33	130/1.39
0.5, 1.3, 4h	122.92/0.75	121.68/0.78	129.05/2.66	127/1.41
0.8, 1.2, 4h	111.42/0.39	113.52/0.57	117.77/1.09	118/0.844
0.8, 1.6, 1h	128.46/0.47	131.28/0.73	154.10/4.35	137/1.48
0.8, 1.5, 2h	137.28/1.64	134.65/1.60	149.79/7.42	142/4.12
0.8, 1.4, 4h	141.65/4.76	135.95/3.49	141.20/8.60	143/10.5

Authors

Zoran R. Radaković was born in Belgrade, Serbia, in 1965. He received his B.S., M.S., and Ph.D. degrees in electric power engineering from the University of Belgrade, School of Electrical Engineering, in 1989, 1992, and 1997, respectively. He has been working as a full professor at the University of Belgrade since 2008. He was a Research Fellow of Alexander von Humboldt-Foundation at the University of Stuttgart from 2001 and 2022. He was working as an R&D engineer in the field of power transformers thermal problems, at Siemens AG from 2004 – 2007 in Nuremberg, Germany.

His professional experience spans R&D, consultancy, and software development across various domains of electrical power, control engineering, and signal processing.

Throughout his academic and professional career, Dr. Radaković has received numerous accolades. He was a recipient of the prestigious "Top Student" scholarship from the Serbian Academy of Sciences and Arts, Belgrade, and was honored as the student of his graduating generation. His Ph.D. dissertation received an award from the Chamber of Economy of Belgrade in 1997. He participated in numerous engineering professional and academic chambers and boards.

Marko V. Novković was born in Pančevo, Serbia, in 1995. He received the B.S. and M.S. degrees in electrical and computer engineering from the University of Belgrade – School of Electrical Engineering, Belgrade, Serbia, in 2018 and 2019, respectively. He is currently pursuing the Ph.D. degree in electrical and computer engineering at the same institution.

Since 2018, he has been Teaching and Research Assistant with the Department of Power Converters and Drives, University of Belgrade – School of Electrical Engineering. His research interests include power transformers, thermal modeling, and electrical heating.

temperature rise. The overshoot in the hot-spot to bulk top-oil temperature difference strongly depends on the micro-location of the temperature sensor measuring the bulk top-oil temperature, as presented in [4].

This chapter presents, for the 370 MVA LIPT, the maximum hot-spot temperature in the HV winding and aging for daily (24h) load diagrams with different short-term overloads – from the steady-state at the pre-load I1 (p.u.), to the load I2 (p.u.), of duration t (h); p.u. loads are with respect to the rated power of 370 MVA. The loading scenarios were selected according to the tables in [8], aiming for relative daily aging around 1 (the first six scenarios in Table 4) or a hot-spot temperature near 140°C (the last three scenarios in Table 4). Standard [8] was used solely to define these loading patterns, while calculations were performed using the THNM, Annex G [6], and IEC [5] models. Annex G of IEEE [6] is more physically based than the IEC model [5], yielding results that closely align with those of the THNM. In contrast, the IEC model [5] shows significant discrepancies compared to the THNM and Annex G models. The IEC model leads to significantly higher aging values. This may be a consequence of adapting the typical values of time constants, which might differ from real values. In this case, the IEC model overestimates the time delay (as the real time constant of the winding is smaller than the applied typical value). As stated in Chapter 5.1, some parameters

of the IEC and Annex G models were determined for a specific transformer, while for other parameters, typical values are used. Better parametrization of the IEC model might lead to aging values similar to those obtained by THNM and Annex G models. The point of the previous discussion is that the estimated aging depends not only on the aging laws (aging versus moisture, oxygen, acids), but also on the thermal models used for determining the temperatures under variable loading grid conditions.

Bibliography

[1] M. Novkovic, F. Torriano, P. Picher, Z. Radakovic, *Application of Dynamic Detailed Thermal Hydraulic Model on a Transformer with Zig-Zag Winding Scale Model*, IEEE Trans. Power Deliv., Vol. 39, No. 6, pp. 3338–3346, 2024, DOI: https://doi.org/10.1109/TPWRD.2024.3466297.

[2] Z. Radakovic, M. Sorgic, *Basics of Detailed Thermal-Hydraulic Model for Thermal Design of Oil Power Transformers*, IEEE Trans. on Power Deliv., Vol. 25, No. 2, pp. 790-802, 2010, DOI: https://doi.org/10.1109/TPWRD.2009.2033076.

[3] *HoST Calculus Software*. Available online: https://www.hostcalculus.com (accessed on 09.09.2025.)

[4] Z. Radakovic, P. Picher, M. Novkovic, F. Torriano, *Dynamic Thermal Digital Twin of Liquid-Immersed Power Transformer*, IEEE Access, Vol. 13, pp. 153308-153319, 2025, DOI: https://doi.org/10.1109/ACCESS.2025.3604720.

[5] Power Transformers – Part 7: Loading Guide for Mineral-Oil-Immersed Transformers, IEC Standard 60076-7, 2017.

[6] IEEE Guide for Loading Mineral-Oil-Immersed Transformers and Step-Voltage Regulators, IEEE C57.91-2011, 2012.

[7] CIGRE Technical Brochure 659, *Transformer thermal modeling*, Working Group WG A2.38, June 2016, ISBN: 978-2-85873-362-0

[8] Loading Guide for Mineral-Oil-Immersed Transformers, IEC Standard 60354, 1991.

Authors

Patrick Picher has been working as a researcher and project manager at Hydro-Québec's Research Institute (IREQ) since 1999. Since 2021, he has also been an adjunct professor with the Université du Québec à Chicoutimi (UQAC). His research interests are mainly focused on diagnostics, monitoring, and modeling of power transformers. Since 2003, he has been involved in many international CIGRE and IEC working groups. He was Secretary of CIGRE Study Committee A2 (transformers) from 2010 to 2016 and the Canadian representative on this committee from 2016 to 2022. He graduated from Sherbrooke University, Canada, in 1993 with a B.Eng. in electrical engineering and received his Ph.D. degree from École Polytechnique de Montréal, Canada, in 1997. Mr. Picher is a member of IEEE (Senior Member), CIGRE (Distinguished Member), and IEC TC 14 (Canadian mirror committee).

Federico Torriano received the B.Sc. degree in physical engineering and the M.Sc. degree in mechanical engineering from Laval University, Québec, Canada, in 2004 and 2006, respectively. In 2007, he joined Hydro-Québec Research Institute, Varennes, Canada, as a researcher and has worked in the field of thermal and fluid analysis of hydroelectric generators and power transformers since then. In 2013, he also started investigating oil-water gravity separators performance through multiphase flow simulations. His research interests include CFD simulation, cooling of large electrical equipment and oil-water gravity separators. He was an active member of the CIGRE A2.38 working group on transformer thermal modeling and he is currently a member of the CIGRE A2.60 working group on dynamic thermal behaviour of power transformers.

PEER REVIEWED

To be continued in the next issue